

Low-Energy-Consumption CO₂ Capture by Liquid–Solid Phase Change Absorption Using Water-Lean Blends of Amino Acid Salts and 2-Alkoxyethanols

Hui Li, Hui Guo, and Shufeng Shen*

Cite This: *ACS Sustainable Chem. Eng.* 2020, 8, 12956–12967

Read Online

ACCESS |



Metrics & More



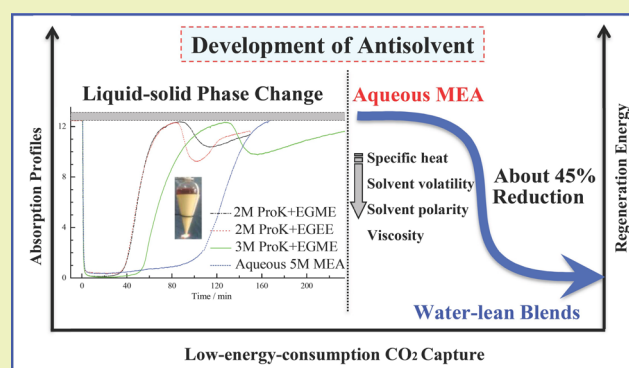
Article Recommendations



Supporting Information

ABSTRACT: Solvent regeneration for the conventional aqueous amine-based CO₂ capture is very energy intensive. Development of phase-changing absorbents is an attractive solution for low energy consumption. In this work, a novel water-lean amino acid salt-based biphasic absorbent was proposed to improve CO₂ capture performance and energy efficiency. Potassium proline (ProK) and potassium sarcosinate (SarK) with a secondary amino group were used as active components, and 2-alkoxyethanols with low volatility, low specific heat, and low viscosity were used as physical antisolvents and triggered the formation of solid phase during CO₂ absorption. CO₂ absorption and desorption characteristics in these systems and continuous capture cycles were investigated under ambient pressure. Relative regeneration energy consumption for solvent regeneration was also evaluated in comparison with the benchmark aqueous MEA. Phase change behavior and partition of CO₂ absorbed in liquid and solid phases were characterized, and the product species in CO₂-rich solid phase were identified by ¹³C NMR and XRD. Results demonstrated that using weak polar solvents, such as 2-methoxyethanol (EGME) and 2-ethoxyethanol (EGEE), can be favorable for the formation of solid precipitates in these systems investigated. Solid slurry with CO₂ loading of 2.5–3.5 mol kg^{−1} can capture about 50–80% of the absorbed CO₂. Ionic products such as bicarbonate and protonated amino acid salt were proved to be the main compositions in the solid precipitate. In comparison with aqueous 5.0 M MEA, the 3.0 M ProK/EGME system showed comparable cyclic capacity (about 0.80 mol kg^{−1}) and a little higher desorption efficiency. Surprisingly, about 40–50% reduction of regeneration energy indicates that water-lean phase change ProK/EGME absorbent has a great potential for advanced CO₂ capture technology.

KEYWORDS: CO₂ capture, Phase change solvent, Potassium proline, Potassium sarcosinate, 2-Alkoxyethanol, Regeneration energy



INTRODUCTION

Global climate change, primarily caused by carbon dioxide (CO₂) emissions, has become a significant environmental issue. One of the promising solutions for effective CO₂ reduction is carbon capture, utilization, and storage (CCUS), which has been the most active research area in recent years. Although adsorption via porous solid adsorbents such as nitrogen-doped carbons^{1,2} and metal–organic frameworks³ has been reported as a promising technology with excellent CO₂ uptake and stability, chemical absorption with amine-based solvents is still the most widely studied among the current capture technologies, and aqueous 30 wt % monoethanolamine (MEA) is the benchmark absorbent for this technology.⁴ However, severe amine degradation and high energy consumption due to high specific heat and enthalpy of vaporization of water solvent are the main hindrances of large-scale CCUS implementation.⁵ To address this issue, extensive research has focused on the design and development of more efficient methods for CO₂ removal from various emission

sources such as flue gas treatment, biogas upgrading, and natural gas processing.⁶

Several advance technologies have been recently proposed, including catalyzed solvents, including enzymes⁷ or solid acids,^{8,9} microencapsulated liquid solvents,¹⁰ polarity-swing-assisted solvents,¹¹ phase change solvents,^{12–15} and ionic liquids.¹⁶ Among these, phase change absorbents have recently gained particular attention.¹⁴ Since a homogeneous solution can undergo a phase transition into a biphasic system during CO₂ absorption and the absorbed CO₂ can be concentrated into one phase, it should have potential to significantly reduce

Received: May 12, 2020

Revised: July 4, 2020

Published: August 11, 2020



Table 1. Physicochemical Property Data of Solvents^{39,40}

solvent	CAS no.	molar mass (g·mol ⁻¹)	ρ /kg·m ⁻³ (303 K)	η , mPa s (303 K)	H_{CO_2} at 303 K, kPa m ³ kmol ⁻¹	boiling point at 101.3 kPa, K	$\Delta_{\text{vap}}H$ (bp), kJ kg ⁻¹	specific heat (C_p), kJ kg ⁻¹ K ⁻¹	vapor pressure at 293 K, Pa	dielectric constant ϵ at 293 K
2-methoxyethanol	109-86-4	76.10	955.5	1.3858	811	397.3	493.3	2.25	1000	17.2
2-ethoxyethanol	110-80-5	90.12	921.0	1.6445	896	408.2	435.2	2.34	500	13.4
dimethylformamide	68-12-2	73.09	944.5 ^a	0.794 ^a	551 ^a	426.2	525.2	2.14	390	38.3
ethylene glycol	107-21-1	62.07	1106.3	13.659	2699	470.5	813.6	2.39	7.4	41.4
ethanol	64-17-5	46.07	781.0	0.981	1031	351.4	837.0	2.44	5899	25.3
water	7732-18-5	18.02	995.7	0.799	3321	373.2	2256.4	4.18	2339	80.1

^aData were obtained at 298 K.

energy consumption by regenerating only the CO₂-rich phase. According to the nature of the new phase, these systems can be divided into two categories: namely, a liquid biphasic system and a liquid–solid phase change system. Some representative liquid biphasic systems, such as mixed amines,^{17,18} polyamines,¹⁹ amines/sulfolane/water,^{20,21} amines/alcohols/H₂O blends,^{22,23} alkanolamine/glymes,²⁴ or their blends with H₂O,²⁵ have been proposed for energy efficient CO₂ capture.

Liquid–solid phase-change absorption has been paid considerable concerns in recent years. Due to the formation of solid precipitates, the CO₂ absorption performance can be enhanced by removing CO₂-loaded products to shift the equilibrium of CO₂ absorption. Some blend systems have been recently reported, such as amine blends in nonaqueous solvents of ethylene glycol or 1,2-propanediol with either methanol or ethanol;²⁶ triethylenetetramine/ethanol blend;²⁷ triethylenetetramine/polyethylene glycol blend;²⁸ linear polyamines in ethanol, diethylene glycol dimethyl ether, *N*-methylpyrrolidone, or dimethyl carbonate;^{29,30} piperazine/*N,N*-dimethylformamide solution;³¹ and potassium proline/ethanol/water solution.³²

Among the above-mentioned biphasic systems, the main reactive compositions are amines and polyamines. Amine degradation is still a problem. Amino acid salts (AAS) such as potassium proline (ProK),^{33,34} potassium sarcosinate (SarK),³⁵ and potassium lysinate³⁶ are of great interest as reactive components for CO₂ capture due to several advantages such as low volatility, resistance to degradation,^{37,38} and fast kinetics.³⁹ Precipitation regime for some amino acid salts in aqueous solution were investigated, and the solid precipitates, resulting from their limited solubility in solutions, were found to be either bicarbonate or zwitterion precipitate.⁴⁰ However, the corresponding processes have a limiting window of operation for precipitation regime.^{41,42} In our previous work, using ethanol partially replacing water was proposed to form a liquid-to-solid precipitating system.³² Proline–ethanol solvent showed faster absorption rate of CO₂ (about three times higher) than aqueous proline solution,⁴³ and about 55–60% of the total CO₂ captured was enriched in the solid phase. The resulting species, i.e., proline carbamate, bicarbonate, and ethyl carbonate salts, in the solid phase were identified by ¹³C NMR and XRD analyses.³² Interestingly, we did not find the precipitates in the system of ProK/ethylene glycol (EG)/water under the postcombustion capture conditions.⁴⁴ The challenge of super high viscosity after absorbing CO₂ for this system was also highlighted. More recently, an aqueous-based solvent composed of potassium glycinate and dimethylformamide (DMF) was proposed to improve the energy efficiency of CO₂ capture.⁴⁵ DMF was used as physical solvent, and its effect on phase change

behaviors was discussed. Introduction of organic solvents into these systems has affected the absorption behavior in different ways, and polarity of solvents might play an important role for the occurrence of CO₂-loaded precipitate. Therefore, development of superior antisolvents is of great interest in this area.

It is worth noting that the use of ethanol and EG to dissolve the CO₂ carrier seems not to be practical for industrial application due to significant solvent loss or poor mass transfer of CO₂ at absorber conditions. Moreover, the increasing hydrolysis of DMF needs to be considered under the basic conditions. Compared with other solvents, 2-alkoxyethanols such as 2-methoxyethanol (EGME) and 2-ethoxyethanol (EGEE) have attractive properties such as low volatility, low specific heat and low viscosity and provide potential advantages as for saving regeneration energy, as shown in Table 1.^{46,47} It was also found that solubility of CO₂ in EGME is much greater than that in water.⁴⁸ A nonaqueous blend of MEA and EGME has been proposed for CO₂ removal from biogas upgrading and natural gas processing in our recent work.^{49,50} However, to the best of our knowledge, using 2-alkoxyethanols as physical antisolvents has not been reported for phase change systems to improve CO₂ capture performance. It is also noted that 2-alkoxyethanols has weak polarity (e.g., $\epsilon = 17.2$ for EGME), thus they can not ionized well the ionic products as well as strong polar water solvent ($\epsilon = 80.1$), which may be in favor of the phase change occurrence. Moreover, phase separation and the compositions in solids might be quite different from other systems for solvent regeneration, which affect the regeneration energy consumption and need to be revealed in detail.

In this work, we have proposed water-lean AAS/2-alkoxyethanol solutions as chemical absorbents to capture CO₂. Potassium proline (ProK) and potassium sarcosinate (SarK) were used for the main compositions in the absorption systems, and EGME and EGEE were used as physical antisolvents to trigger the liquid–solid phase change. Water is only from the neutralization reaction of amino acid with potassium hydroxide (KOH) and no additional water was added in these systems. CO₂ absorption and desorption characteristics in the above-mentioned systems were performed under ambient pressure and compared with conventional aqueous 5.0 M MEA. Phase behaviors and partition of CO₂ absorbed between liquid and solid phases were characterized, and the product species were identified by ¹³C NMR and XRD. The stability of the absorbents after several absorption and desorption cycles and the relative energy consumption were evaluated at 373 K.

EXPERIMENTAL SECTION

Chemicals and Materials. L-Proline (Pro, 99.28% HPLC purity, CAS no. 147-85-3), sarcosine (Sar, 98.24% HPLC purity, CAS no.

107-97-1), monoethanolamine (MEA, 99.12% GC purity, CAS no. 141-43-5), potassium hydroxide (KOH, 95% GR, CAS no. 1310-58-3), 2-methoxyethanol (EGME, 99.89% GC purity, CAS no. 109-86-4), and 2-ethoxyethanol (EGEE, 99.18% GC purity, CAS no. 110-80-5) were purchased from Aladdin Reagent, China. All of chemical reagents were used without further purification. N₂ (99.99%, v/v) and CO₂ (99.995%, v/v) were obtained commercially from Shijiazhuang Xisanjiao Oxygen Generation Station. Pure N₂, CO₂, and standard mixed gas (19.98% CO₂ balanced with N₂) from Nanjing Special Gas Factory Co., Ltd., were used for calibration of nondispersive infrared (NDIR) CO₂ gas analyzers (GXH-3011N, 0–20%, uncertainty 1.0% FS, Institute of Beijing Huayun Analytical Instrument; SKS-BA-CO₂, 0–100%, uncertainty 1.0% FS, Guangdong Skesen Gas Detection Equipment Co., Ltd.). Electronic analytical balances (OHAUS, CP214, Scout SE 1501F) were used for weight measurements. The absorbent solutions were prepared by dissolving amino acid in solvent (EGME or EGEE) with an equimolar amount of KOH in a volumetric flask at 293 K.

CO₂ Absorption. Screening experiments were performed to investigate CO₂ absorption behavior and capacity of different absorbent systems at near atmospheric pressure. A similar experimental apparatus and the method were described in detail in our previous work.^{32,44} Schematic diagram can be found in the Supporting Information (SI), Figure S1. Before CO₂ absorption experiments, CO₂ analyzer was calibrated by pure N₂ and standard gas. A gas mixture of N₂/CO₂ (13.0 ± 0.5 vol % CO₂) with a total flow rate of 540 mL min^{−1} was sent through a 250 mL glass reactor immersed in a water bath (DF-101S), and followed by a Graham condenser (C544300, Synthware, Beijing). Then the gas stream entered into the online CO₂ analyzer after a drying tube. The CO₂ concentration in the mixture was recorded along the elapsed time. A known mass (150 mL) of preheated solution was injected into the reactor to start the absorption. A magnetic stirrer at a constant speed was used to improve the liquid–gas contact, especially for the case of solid precipitate formation. Samples were taken when the outlet CO₂ concentration reached 95% of the inlet CO₂ concentration. It should be pointed out that the CO₂ content in the outlet gas stream would decrease significantly when the solid precipitates formed and then increase gradually. Absorption would not stop until the CO₂ concentration in the outlet stream was the same as that in the inlet. The profiles of CO₂ concentration in the outlet gas stream could be obtained by the recorded data from online CO₂ analyzer. Average absorption rates in mol kg^{−1} s^{−1} for different absorbents were calculated in the first 20 min and the method can be found in the SI.

Samples were taken again after the absorption test for the measurement of CO₂ loading by a modified Chittick CO₂ apparatus.³² After sampling the slurry from the liquid–solid system, phase separation was enhanced by a TDZ4-WS Centrifuge (Hunan Herexi Instrument, China) at 3800 rpm for 60 min. CO₂ absorbed in the liquid top phase and solid precipitates was analyzed.

CO₂ Desorption Experiment. After CO₂ absorption, the performance of CO₂ desorption was estimated by a widely used gas-stripping method,^{44,49,51,52} as shown in Figure S1. The reactor with CO₂-loaded solution was removed overhead and back to the water bath when the temperature 353 K was reached. CO₂ desorption was started by bubbling pure N₂ as a carrier gas at a flow rate of 0.2 L/min through the CO₂-loaded solutions. The CO₂ content in the mixture could be monitored by the CO₂ analyzer (SKS-BA-CO₂). Desorption was stopped until the CO₂ concentration was below 2%. Generally, the CO₂-released solution became homogeneous CO₂-lean liquid and then liquid samples were taken. The desorption profiles were obtained by the logged concentration data from online CO₂ analyzer. Average desorption rates in mol kg^{−1} s^{−1} were also calculated in the first 20 min (see the SI).

The CO₂ cyclic capacity is defined by the difference between rich loading after absorption and lean loading after desorption, with units in mole CO₂ per kg CO₂-free solution.

$$\Delta\alpha = \alpha_{\text{rich}} - \alpha_{\text{lean}} \quad (1)$$

Continuous Cycles of Absorption–Desorption Experiment.

The feasibility of phase change absorbents was investigated by means of several continuous cycles of absorption (313 K)–desorption (353 K) tests in order to give assessments of long-term solvent behavior and CO₂ cyclic capacity ($\Delta\alpha$). In order to reduce the solvent loss, the slurry solution was not separated for the desorption step after CO₂ absorption. Moreover, the CO₂ lean solution was used for the next absorption–desorption cycle. One batch of complete cyclic experiment lasted about 5.5 h. CO₂ loading (α) of solutions was measured before and after CO₂ absorption to obtain the CO₂ cyclic capacity for each run.

Evaluation of Relative Energy Consumption for Phase Change Solvents.

A thermal regeneration method was used to measure the overall electric energy during CO₂ desorption for various absorbents at 373 K. No purge gas was used. The apparatus (shown in Figure S2) and the method were reported in our previous work.^{49,53} In this work, overall electric energy (E_T) required for solvent regeneration was recorded using an energy meter (eSensor, Altenergy Power System Inc., China, stated accuracy of 0.001 kWh). The flow rate and the cumulative volume of CO₂ released at standard conditions were recorded by a CO₂ mass flow meter (CS200A, 0–3.7 L min^{−1}, Beijing Sevenstar Flow Co., Ltd., China). Only a brief operating procedure presents here. 1.8 L of CO₂-free absorbent solution was used for CO₂ absorption under 15% CO₂ partial pressure to obtain CO₂-saturated solution at 313 K. Then, the CO₂-loaded solution was heated from 313 to 373 K for CO₂ desorption. When the temperature was raised to 343 K where CO₂ was initially released from the solution, the energy meter and flow meter started to record the data. The whole process lasted for about 2.0 h. Aqueous 30% (SM) MEA was used as a baseline case for assessment of regeneration energy consumption.

Due to the formation of liquid–solid phase change, the slurry mixture was gravitationally settled for 2 h for solid–liquid separation and then most of CO₂-lean phase (about 0.5L) was removed. CO₂-rich slurry was desorption at 373 K. The slurry mixture without phase separation was also measured in order to eliminate the effect of volume change on overall heat loss. In some cases, the resultant CO₂-lean solutions, referred as the blank systems, were performed the same desorption procedure again to obtain the energy required without CO₂ desorption (E_0 or H_0). It was noted that the heat dissipation was not estimated separately and was lumped into the measured overall electric energy.

The regeneration energy consumption (Q_{reg}) is expressed as the cumulative heat requirement (H_T) divided by the total amounts of CO₂ released (m_{CO_2}) in the first 30 min, the unit in GJ t^{−1} CO₂ or kJ kg^{−1} CO₂ released. It was assumed that conversion efficiency of electricity-to-heat ($E-H$) energy was 75% in this work. The relative energy consumption (RE, %) was used for evaluating regeneration energy consumption for phase change systems, which is defined as the Q_{reg} for the phase change systems divided by that for the baseline case in the first 30 min during CO₂ desorption.

$$Q_{\text{reg}} = \frac{H_T}{m_{\text{CO}_2}} \quad (2)$$

$$\text{RE, \%} = \frac{Q_{\text{reg},i}}{Q_{\text{reg, baseline}}} \quad (3)$$

Additionally, the regeneration energy consumption can also be estimated by the following equation:

$$Q_{\text{reg}} = Q_1 + Q_2 + Q_3 = \frac{m_m C_{p,m} \Delta T + (H_T - H_0)}{m_{\text{CO}_2}} \quad (4)$$

where Q_1 , Q_2 , and Q_3 are the sensible heat, latent heat of solvent vapor, and desorption heat, respectively. m_m is the mass of the mixture used and $C_{p,m}$ is the estimated specific heat capacity of the mixtures from the pure components at 298 K.⁴⁶ The variation in C_p with temperature for all components was ignored in the present work. ΔT was set to be 10 and 20 K for desorption at 373 and 383 K,

respectively. H_T and H_0 are the heat requirement for the CO_2 -loaded and the corresponding blank solutions in the first 30 min during regeneration process, respectively.

Analytical Methods. The CO_2 loadings of solutions or solid precipitates can be measured by acid titration using a modified Chittick CO_2 apparatus in the SI, Figure S3. The detailed method can be found in the SI. Each sample was determined three times to obtain an average CO_2 loading in mol kg^{-1} . The error of loadings is found to be about $0.005 \text{ mol kg}^{-1}$.

^{13}C NMR spectra were obtained by using a Bruker Avance 500 spectrometer operating at 125.77 MHz. To provide enough signals for the deuterium lock, D_2O was introduced into the NMR tube containing the samples at 298.0 K. The precipitate samples were prepared by centrifuge separation at 12 000 rpm for 10 min and then dried under CO_2 at 283 K. Chemical shifts are given relative to CH_3CN as an internal reference at 1.47 and 119.7 ppm in D_2O .

DSC-TGA experiment was carried out using a SDT Q600 V20.9 Build 20 analyzer. The samples were analyzed at a heating rate of 10 K min^{-1} and N_2 flow rate of 40 mL min^{-1} . The X-ray diffraction (XRD) patterns of precipitate were also collected on a Rigaku D/MAX-2500 XRD system (Cu $K\alpha$ radiation, $\lambda = 0.15406 \text{ nm}$) operated at 40 kV and 150 mA.

RESULTS AND DISCUSSION

CO_2 Absorption and Desorption Characteristics for Different Absorbents. CO_2 absorption (313 K) and desorption (353 K) experiments were investigated for SarK-based and ProK-based absorbents in 2-alkoxyethanol solvents. Variation of the outlet CO_2 concentration and temperature of solutions against the elapsed time were recorded. After CO_2 absorption, the absorption capacity expressed as the final loading, α_{final} , was measured. CO_2 absorption and desorption profiles for two different amino acid salt systems were shown in Figures 1 and 2, respectively, in comparison to conventional aqueous MEA. Comparison of their absorption capacity and cyclic loading capacity at the similar operating conditions was also summarized in Table 2. It is worth pointing out that the water-lean absorbents, prepared by dissolving amino acid in glycol ethers with an equimolar amount of potassium hydroxide, contained a little amount of water from neutralization reaction of the amino acid with the strong base. The measured water content was ranged from 1.6 to 5.8 wt %. Due to the limited solubility of SarK and ProK in water-lean alkoxyethanols, the molar concentrations of these amino acid salts, not greater than 3.0M, were investigated in this work after initial solubility tests.

For SarK-based systems during CO_2 absorption, the outlet CO_2 concentration increased sharply near to the feed value, and then decreased gradually to minima. At this time, the system underwent a liquid-to-solid phase change process in the form of white solid precipitates. The outlet CO_2 concentration increased slightly again back to the equilibrium, as shown in Figure 1a. The trend of absorption curves is similar for 1.0 and 2.0 M SarK in EGME or EGEE. Aqueous 5.0 M MEA showed no phase-splitting behavior and remained homogeneous solution after CO_2 absorption, so different absorption patterns were observed. It was also noted that the absorption capacity increased with the increasing concentration of SarK since amino acid salts acted as reactive components in the solution. However, 2.0 M SarK/EGME absorbent showed very poor absorption capacity (about 0.94 mol/kg) for CO_2 removal, only about 43% of that for aqueous 5 M MEA under the same capture conditions.

As for ProK-based systems, phase change behavior was also observed for all absorbents. When solid precipitates produced,

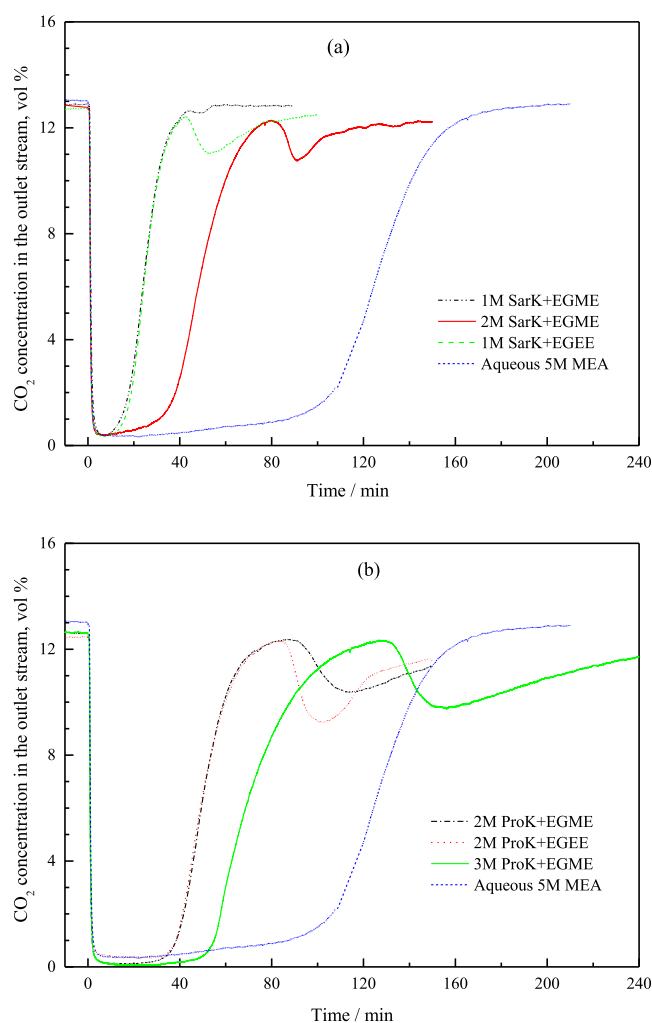


Figure 1. CO_2 absorption profiles (the outlet CO_2 concentration curves versus time) for various water-lean absorbent systems compared with aqueous MEA at 313 K. MEA: monoethanolamine; SarK: potassium sarcosinate; ProK: potassium proline; EGME: 2-methoxyethanol; EGEE: 2-ethoxyethanol. (a) SarK-based systems; (b) ProK-based systems. The CO_2 concentration in the simulated gas mixture was $13.0 \pm 0.5 \text{ mol } \%$.

the solution turned turbid and then the absorption rate of CO_2 was clearly enhanced as a result of sharp decrease in the outlet CO_2 concentration (Figure 1b). Similar to SarK-based system, the formation of solid precipitates can increase about 15–20% absorption capacity. It was also found that the absorption capacity was mainly dependent on the concentration of ProK or SarK. CO_2 may react with the deprotonated secondary amino group in these amino acid salts forming ionic carbamate products and protonated amino acid salts by well-known reaction mechanisms (i.e., zwitterion mechanism and termolecular mechanism). 2-Alkoxyethanols can be considered as nonreactive diluents as components in the mixtures. Therefore, very similar values of absorption capacity were observed for the absorbents with the same concentration and physical solvent under the same capture conditions.

It is interesting to find out that the difference in absorption curves for different blends is quite small before phase change occurs. However, the effect of solvent polarity on phase behavior and CO_2 removal performance is significant after the formation of solid precipitates mainly due to salting-out effect

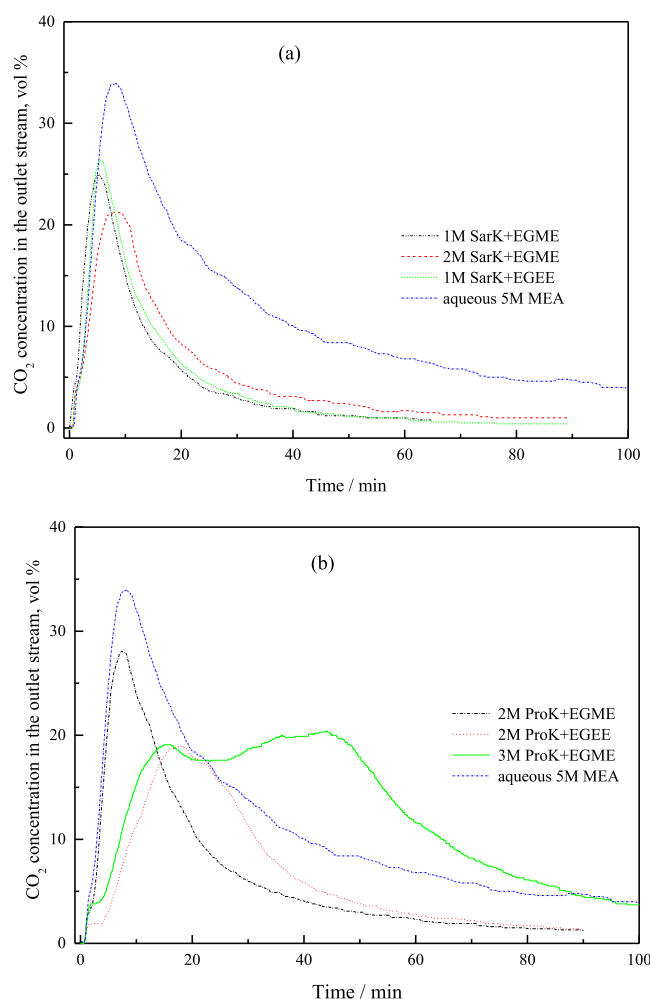


Figure 2. CO₂ desorption curves for different absorbent systems at 353 K with N₂ flow rate of 0.2 L min⁻¹ compared with aqueous 5 M MEA solution. (a) SarK-based systems; (b) ProK-based systems.

of the solvent used. Generally, the lower the dielectric constant of a solvent, the less polar it is. In comparison of EGME solvent ($\epsilon = 17.2$), the resultant hydrophilic absorption products were found to easily precipitate out due to their limited solubility in weaker polar EGEE ($\epsilon = 13.4$). Similar

phenomenon has been reported previously for ProK-ethanol systems.³² Therefore, these results clearly demonstrate that solvents with different polarity can affect the phase change characteristics. Using weak polar solvents will be favorable for the formation of solid phase in these systems investigated. As shown in Table 2, the systems using EGEE as an antisolvent can increase about 5–9% capacity than the EGME-based systems under the same conditions. Although ProK-based absorbent, in particular 3.0 M ProK/EGME, showed excellent absorption efficiency in the first 50 min, its final loading capacity, about 1.75 mol/kg, was still low in comparison with that (about 2.2 mol/kg) for aqueous 5.0 M MEA. The low absorption capacity can be ascribed to the lower molar concentration of amino acid salt than MEA.

Compared with the primary amine group in MEA, the reaction kinetics of secondary amino groups in ProK and SarK is generally slow with CO₂. However, the physical solubility of CO₂ in water-lean glycol ethers is great higher than that for water solvent, which results in high absorption rate in the initial phase of CO₂ absorption. As more CO₂ is chemically absorbed as the carbamate and/or bicarbonate products, the equilibrium partial pressure of CO₂ over the CO₂-loaded solution increases and the driving force of absorption decreases, resulting in the poor removal performance of CO₂ from the gas mixtures. When solid products precipitate out from the solution, the CO₂ loading in the liquid solution will decrease and the equilibrium CO₂ partial pressure will also decrease. Therefore, an increase in the absorption rate of CO₂ was observed because the driving force (i.e., the difference between CO₂ partial pressure of the gas bulk phase and the equilibrium CO₂ partial pressure over the liquid phase) for absorption has a little increase. More CO₂ can be captured into these absorbents. As the active absorbent in the liquid phase depleted, the equilibrium partial pressure of CO₂ over the liquid increased gradually. Thus, the absorption rate of CO₂ decreased, resulting in the increasing concentration of CO₂ in the outlet.

For CO₂ desorption using thermo-assisted gas strip method, it can be seen from desorption profiles that regeneration of SarK-based phase change solutions is easier than aqueous MEA. The average desorption efficiency for SarK-based phase change solutions were about 67% with respect to the absorbed, which is much higher than that (about 39%) for aqueous MEA.

Table 2. Comparison of CO₂ absorption-desorption performance of different absorption systems.^a

absorbent system	CO ₂ absorption				CO ₂ desorption		cyclic loading $\Delta\alpha^c$ mol kg ⁻¹
	$\alpha_{95\%}^b$	T_{Abs}^c	α_{final}	$10^5 R_{Abs}^d$	$\alpha_{2\%}$	$10^5 R_{Des}^d$	
	mol kg ⁻¹	h	mol kg ⁻¹	mol kg ⁻¹ s ⁻¹	mol kg ⁻¹	mol kg ⁻¹ s ⁻¹	
1 M SarK + EGME	0.401	1.5	0.406	28.88	0.082	16.54	0.324
2 M SarK + EGME	0.812	2.5	0.943	29.06	0.403	22.79	0.540
1 M SarK + EGEE	0.439	2.5	0.535	29.56	0.192	19.19	0.343
2 M ProK + EGME	0.817	2.5	0.954	28.64	0.516	29.20	0.438
2 M ProK + EGEE	0.859	2.5	1.046	28.63	0.577	18.32	0.469
3 M ProK + EGME	1.545	5.0	1.749	31.14	0.930	14.86	0.819
aqueous 3.3 M MEA		2.5	1.570	-	0.938	-	0.632
aqueous 5 M MEA	2.180	3.5	2.198	30.84	1.357	32.67	0.841

^a α is defined as the moles of CO₂ per kg of CO₂-free sample solution, mol kg⁻¹. The standard uncertainties u are $u(\alpha) = 0.005$ mol kg⁻¹, $u(10^5 R) = 0.03$ mol kg⁻¹ s⁻¹. ^b $\alpha_{95\%}$ is the CO₂ loading when CO₂ content in the outlet gases is 95% of that in the inlet gas mixture. ^c T_{Abs} is the total absorption time. ^d $10^5 R_{Abs}$ and $10^5 R_{Des}$ are the CO₂ absorption and desorption rate in the first 20 min, respectively. ^eCyclic loading $\Delta\alpha$ was calculated by the difference between rich loading after absorption α_{final} and lean loading after desorption $\alpha_{2\%}$, with units in mole CO₂ per kg CO₂-free solution.

However, the SarK concentration was far lower than the MEA concentration in these runs, resulting in low cyclic loading in mol kg^{-1} for Sark-based systems. The average desorption efficiency for ProK-based systems were about 45%, which is a little higher than that for aqueous MEA. It was noted that 3.0 M ProK/EGME had comparable cyclic capacity with aqueous 5 M MEA (Table 2). It should be pointed out that desorption rates in the first 20 min for all slurry systems were slower than the single-phase MEA system at such a low temperature using gas-stripping method. The increased viscosity and the additional dissolution step of CO_2 -loaded solid may result in low mass transfer coefficient. From the viewpoint of operating cyclic capacity, 3.0 M ProK/EGME and 2.0 M SarK/EGME absorbents with liquid-to-solid phase change were considered in further study.

Regenerability of the absorbents was comprehensively investigated by means of continuous cycles of absorption–desorption to evaluate their reuse performance and long-term stability. Four continuous cycles of absorption (300 min)–desorption (140 min) were performed. The representative absorption and desorption profiles and the measured results for 3.0 M ProK/EGME and 2.0 M SarK/EGME systems were shown in Figure 3. As can be seen, the absorption behavior and cyclic capacity reveal that the absorption (313 K)–desorption (353 K) performance of these absorbents is relatively stable for the reused solvents, considering the first cycle using the fresh solution and the measuring uncertainty of CO_2 loading. Under the specific operating conditions, the absorption capacity was maintained at about 1.75 $\text{mol CO}_2/\text{kg}$ for ProK/EGME system and 0.95 $\text{mol CO}_2/\text{kg}$ for SarK/EGME system. The cyclic capacity was about 0.82 and 0.52 $\text{mol CO}_2/\text{kg}$ for ProK/EGME and SarK/EGME systems respectively, which is also consistent with results in Table 2. As known that the cyclic capacity for the most used 5.0 M MEA was about 1.0 $\text{mol CO}_2/\text{kg}$ under the absorption (313 K)–desorption (393 K) conditions.^{22,54} Thus, the potential for reducing energy consumption using these phase change absorbents are also highly interested in developing energy efficient CO_2 capture process.

Phase Separation and Solid Precipitate Analysis. As mentioned above, Sark-based and ProK-based absorbent systems can produce phase change and form slurry solutions after CO_2 absorption. To quantify the performance of phase separation, the slurry was separated by centrifuge in centrifugal tubes at 3800 rpm for 60 min and two distinct phases appeared, i.e. a liquid top phase and a solid bottom phase. The typical pictures before and after CO_2 absorption are presented in SI Figure.S4. Two phases were separated and then weighted. Samples were taken from each phase and the analytical results are presented in Table 3. It was noted that 3.0 M ProK/EGME solution produced many fine solid particles after CO_2 absorption and the slurry was not completely separated at 2000 rpm for 20 min.

It was found that the upper and the lower phases exhibit a huge difference in CO_2 loading, and the amount of the obtained solid phase (defined as the mass fraction between the solid phase and the total) is in the range of 14–30 mass %, which can captured about 50–90% of the total absorbed CO_2 . The very low CO_2 loading in top phase indicates that the ionic reaction products have low solubility in EGME or EGEE solvent. 2-alkoxyethanols can be used as superantisolvents in these systems. Therefore, these results clearly demonstrate that the absorbed CO_2 can be enriched in the solid phase. High

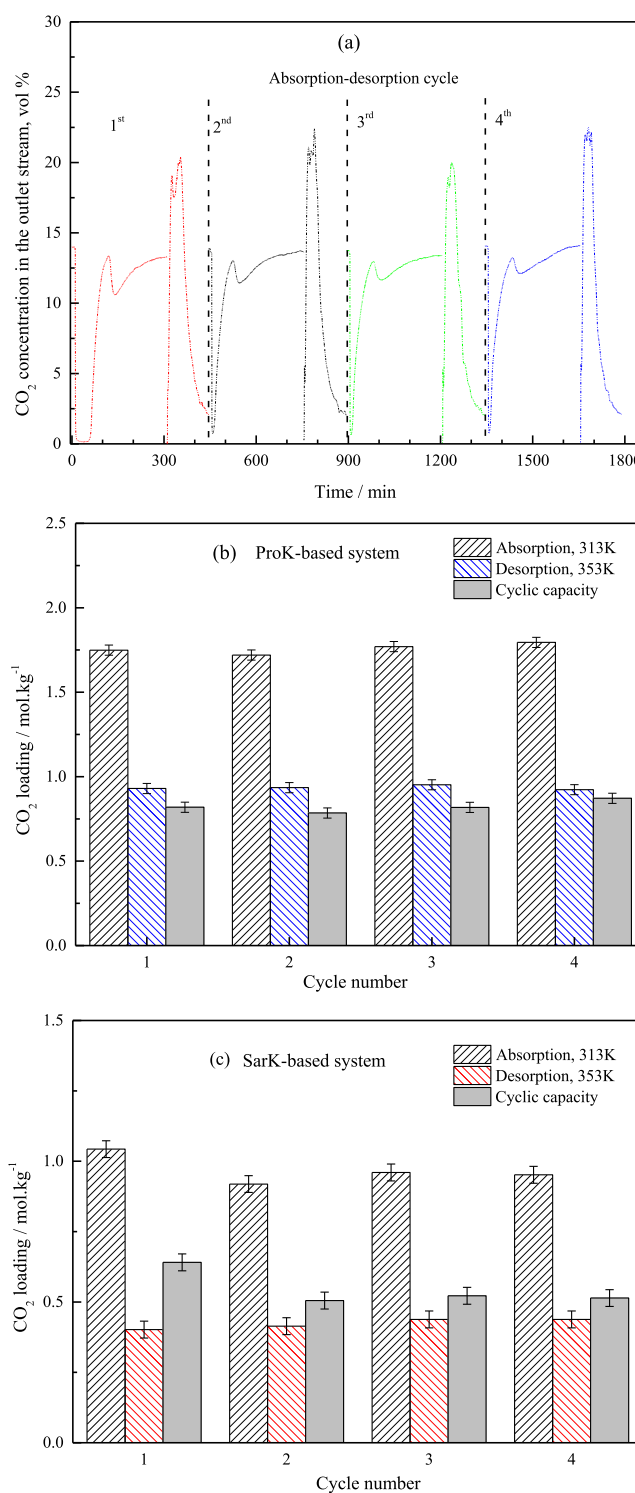


Figure 3. Absorption (313 K)–desorption (353 K) cycling runs of water-lean absorbents. (a) The representative profiles of continuous absorption–desorption runs for 3 M ProK+EGME system; (b) Cyclic capacity of 3 M ProK+EGME system. (c) Cyclic capacity of 2 M SarK-based system. Absorption was performed using the simulated gas mixture with 13.0 mol % CO_2 and desorption was carried out by a gas stripping method at 353 K and 0.2 L min^{-1} N_2 flow rate.

enhancement factor can be a promising signal for phase change systems. In a practical sense, CO_2 -rich solid or slurry phase may be sent to a stripper for solvent regeneration and the CO_2 -lean liquid phase, without thermal regeneration, can be used

Table 3. CO₂ Distribution in Solid and Liquid Phases after Absorption for Different Systems^a

absorbent system	liquid phase		solid phase		captured CO ₂ in solid phase, %
	mass %	α liquid, mol/kg	mass %	α solid, mol/kg	
1 M SarK + EGEE	71.0	0.094	29.0	1.973	89.6
	70.9	0.102	29.1	2.153	89.6
2 M SarK + EGME	82.7	0.551	17.3	3.046	53.6
2 M ProK + EGME	85.3	0.625	14.7	3.480	49.0
2 M ProK + EGEE	85.1	0.626	14.9	3.566	50.0
	77.0	0.567	23.0	3.302	63.5
2 M ProK + EGEE	76.8	0.571	23.2	3.108	62.2
	50.8	0.748	49.2 ^b	2.574	77.0
3 M ProK + EGME ^b	47.9	0.732	52.1 ^b	2.527	79.0

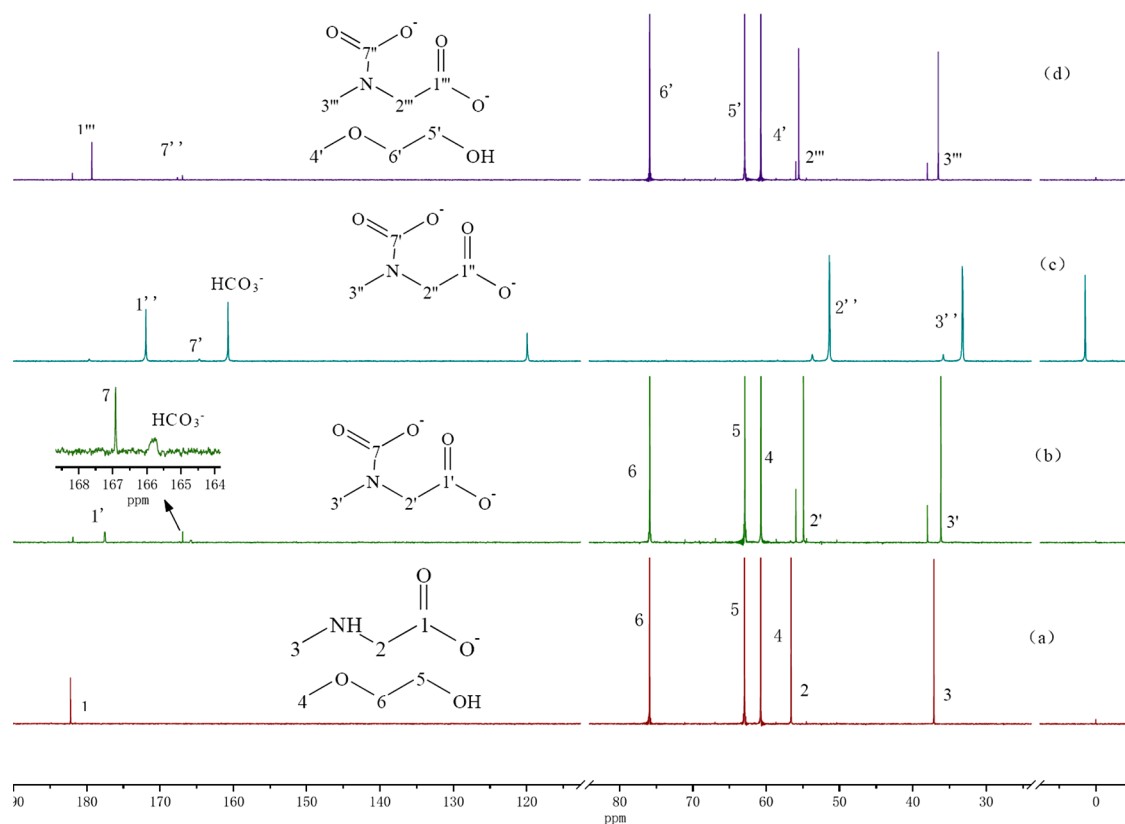
^a α is defined as the moles of CO₂ per kg of sample solution, mol kg⁻¹, and phase separation was enhanced by the centrifuge at 3800 rpm for 60 min. The standard uncertainties u are $u(\alpha) = 0.005$ mol kg⁻¹. ^bFor this absorbent, phase separation was enhanced by the centrifuge at 2000 rpm for 20 min, and the bottom slurry phase contained a small amount of liquids.

for dissolution of regenerated solid and sent back to absorption column as lean absorbent. The higher mass fraction of the liquid phase, the more energy saving for solvent regeneration will be. The benefit of phase separation can also be verified in the next section.

The qualitative ¹³C NMR analysis was further performed to identify the main species in the resultant solutions and the solid precipitates after CO₂ absorption. NMR spectra of 2.0 M

SarK/EGME and 3.0 M ProK/EGME systems in D₂O are shown in Figures 4 and 5, respectively. Three samples, i.e. fresh solution, CO₂-loaded solution before phase change and dried solid, were tagged as (a), (b), and (c) in the figures. Peak assignment was performed according to the literature data.^{32,55–57} The detailed chemical shifts of ¹³C NMR spectra can be found in SI, Tables 1–2.

As shown in Figure 4a, the nonequivalent C atoms of SarK and EGME are labeled #1–6. After CO₂ absorption, “doubled” signals for nos. 1–3 carbons appeared and two new signals were observed in the range of 165–168 ppm in the early stage of CO₂ absorption (Figure 4b). The peaks at 178 and 182 ppm were assigned to the free sarcosine and protonated sarcosine (SarH⁺), respectively. The chemical shift of about 167 ppm with high signal intensity was assigned to the main product SarK carbamate from the reaction between the secondary amino group of SarK and CO₂, and the very weak peak at 165–166 ppm suggested the formation of bicarbonate-carbonate species from the possible carbamate hydrolysis. The unchanged carbon signals for EGME also indicated that EGME as an inactive solvent was not involved in the chemical reactions. Interestingly, the signal for bicarbonate species at about 161 ppm showed significantly high intensity in comparison with that for carbamate, indicating that bicarbonate is possible to be one of the main compositions in the solid sample as well as protonated sarcosine. The similar phenomena were also observed for 3.0 M ProK/EGME systems. In the sample at CO₂ loading about 1.0 mol CO₂/kg, ProK carbamate was found to be the main product species (#9 carbon peak in Figure 5b). The chemical shift with high intensity in the range of 160–161 ppm was assigned to

**Figure 4.** ¹³C NMR spectra of SarK+KOH+EGME solutions in D₂O. (a) CO₂-free sample, (b) CO₂-loaded solution at $\alpha = 0.653$ mol/kg before phase change, (c) solid precipitate with CH₃CN in D₂O, and (d) samples after absorption–desorption cycles, $\alpha = 0.438$ mol/kg.

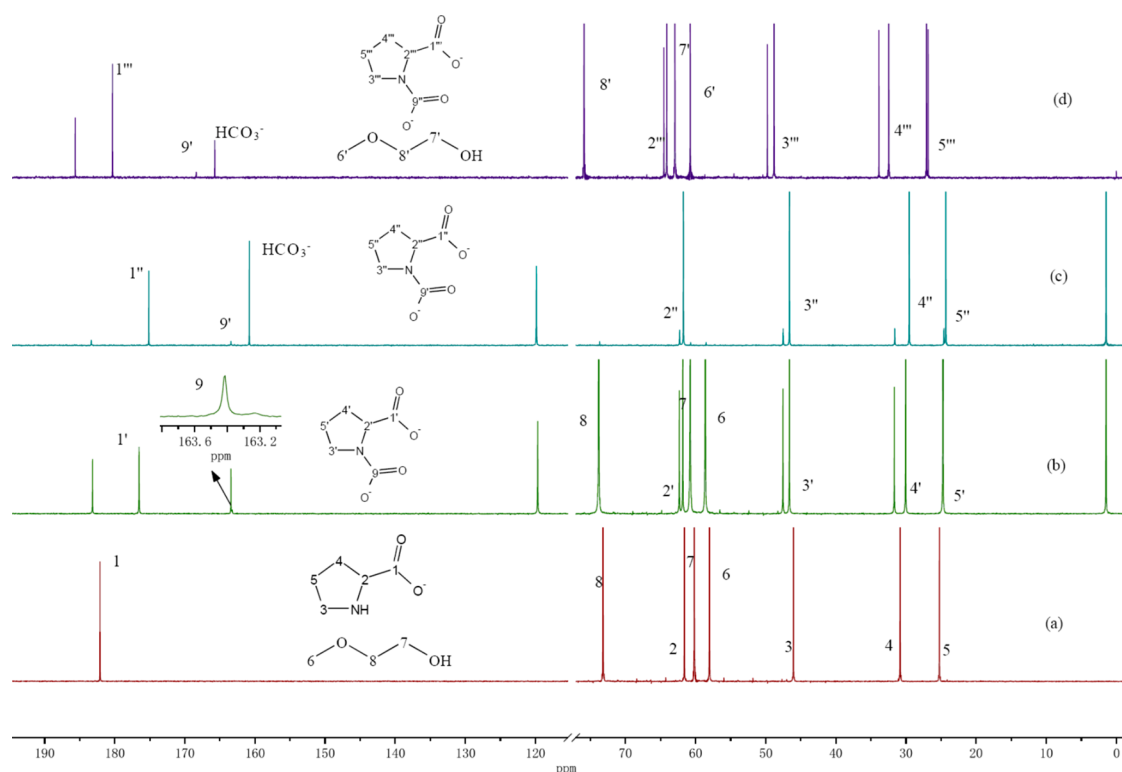


Figure 5. ^{13}C NMR spectra of Pro+KOH+EGME solutions in D_2O . (a) CO_2 -free sample, (b) CO_2 -loaded solution at $\alpha = 1.059$ mol/kg before phase change, (c) solid precipitate with CH_3CN in D_2O , and (d) samples after absorption–desorption cycles, $\alpha = 0.923$ mol/kg.

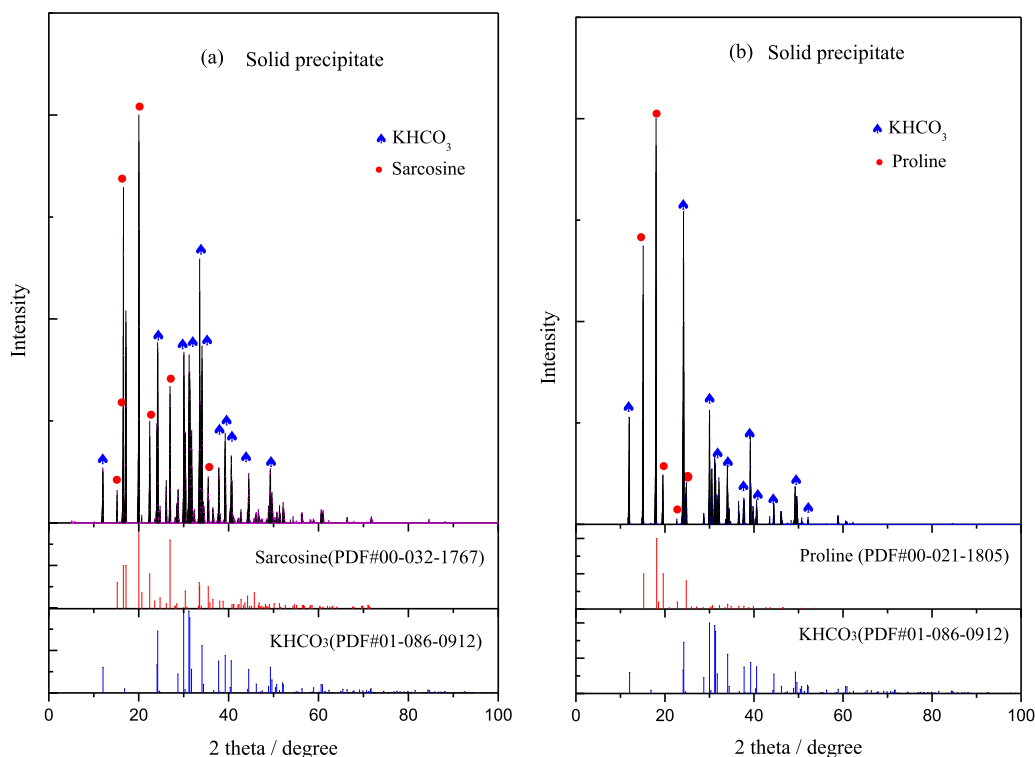


Figure 6. XRD patterns of the solid precipitates generated by CO_2 absorption into water-lean absorbents. (a) solid precipitates from Sar+KOH+EGME solutions and (b) solid precipitates from Pro+KOH+EGME solutions.

bicarbonate product in the solid sample. For the CO_2 -lean samples from the fourth cycle of absorption–desorption in Figures 4d and 5d, weak signals at 167–168 ppm for carbonate species and signals at 165–167 ppm for carbonyl carbon of

carbamates were observed. Notably, no additional carbon signals were observed for the two systems.

The X-ray diffractograms (XRD) of solid precipitates were presented to gain more insight of its compositions in Figure 6.

Sarcosine (PDF no. 00-032-1767), proline (PDF no. 00-021-1805) and potassium bicarbonate (PDF no. 01-086-0912) patterns from the JCPDS database were also included for comparison. These results further demonstrate that the solid phase could be a mixture of bicarbonate and protonated amino acid salts, which is consistent with the findings in NMR analysis.

The decomposition of solid products was studied using DSC-TGA analyzer, as shown in SI, Figure S5. Results indicate that the decomposition of products commences at about 375 K and the decomposition for SarK/EGME system is faster than that for ProK/EGME system. Large endothermic peaks were observed at 390 and 420 K respectively due to the release of large amounts of CO₂ in solids.

These results indicate that, during CO₂ absorption in water-lean AAS absorbents, the resultant products are in the form of amino acid carbamates by amine reaction with CO₂ via zwitterions or termolecular mechanism in the early stage. Carbamate hydrolysis and CO₂ hydration promoted by amino acid salt accelerate greatly with the increasing CO₂ loading, resulting in the formation of bicarbonate/carbonate product. Due to the limited solubility of ionic reaction products in water-lean alkoxyethanols, CO₂-rich solid phase precipitates out and then phase change happens at a certain loading point.

Regeneration Energy Evaluation for Water-Lean AAS-Based Phase Change Absorbents. The representative profiles of accumulative electricity energy, amounts of CO₂ desorbed and temperature along with desorption time for the conventional 5 M MEA (as a baseline case for comparison) and phase change systems at 373 K are presented in Figures 7 and 8. The more detailed information in the 2 h period is also shown in SI, Figure S6.

It can be seen that, the released amounts of CO₂ and energy consumption increased greatly for all systems in the first 10 min, moreover about 95% of CO₂ was released from phase change systems at 20 min. However, for the aqueous 5.0 M MEA, the accumulative electricity energy and amounts of CO₂ continued to increase slowly even after 30 min, possibly due to high partial pressure of water vapor over the solution at 373 K and the positive effect of gas flow on mass transfer. The required sensible heat for these water-lean systems was significantly reduced, which can be roughly represented from the energy and temperature profiles in the first 8 min in Figure 8a.

Regeneration energy consumption for water-lean phase change systems was evaluated in two different ways. In the first method reported in literature,^{9,49} the cumulative overall heat requirement (H_T) from the recorded total electricity energy included the sensible heat to reach 373 K from the 343 K (Q_1 , $\Delta T = 30$ K), the latent heat of vaporization (Q_2) of solvent vapor (e.g., water and EGME) leaving the desorber along with the desorbed CO₂, the heat of CO₂ desorption (Q_3) and the associated heat loss (Q_{loss}) due to insufficient insulation in the desorption process. Therefore, the heat dissipation was not estimated separately and was lumped into the total electric energy in this way. In order to minimize the effect of heat loss on the total energy consumption, the recorded data in the first 30 min was used for calculation and comparison, and at this time most of CO₂ was released from the solutions. The estimated energy consumption and the relative total energy consumption is summarized in Table S3 and Figure 7 (b). It is worth noting that the overall electricity energy for water-lean phase change systems is more than 45%

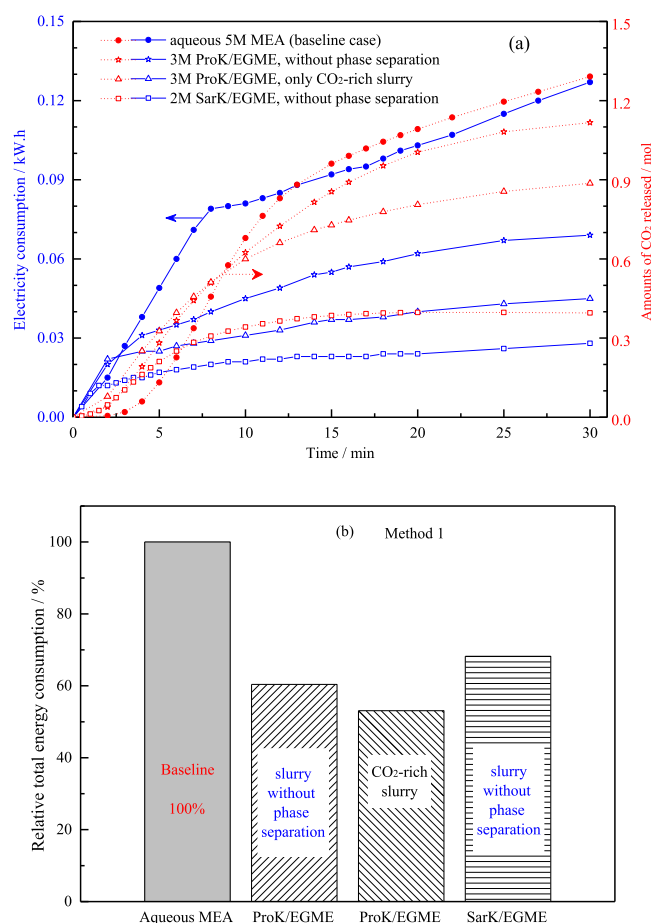


Figure 7. Comparison of energy consumption under thermal desorption conditions at 373 K for CO₂-saturated aqueous and water-lean systems (under 15.0 kPa of CO₂ partial pressure at 313 K). Method 1: (a) Desorption profiles of aqueous 5.0 M MEA, 3.0 M ProK/EGME slurry without phase separation and CO₂-rich slurry, 2.0 M SarK/EGME slurry without phase separation and (b) relative energy consumption for regeneration at 373 K in the first 30 min.

lower than that for aqueous 5.0 M MEA. Take 3.0 M ProK/EGME system for example in Table S3, the overall energy consumption was estimated to be 3720 kJ kg⁻¹ CO₂ for the slurry without phase separation, which is far lower than that (about 6158 kJ kg⁻¹ CO₂) for aqueous 5.0 M MEA. The relative energy consumption (%) was considered as a reliable indicator for comparison under the same operating conditions using the same desorption equipment. About 40% energy reduction for phase change ProK/EGME system was observed in the initial assessment. As mentioned in the absorption section, after phase separation for phase change systems, the CO₂ absorbed is concentrated into solid phase, thus only the regeneration of CO₂-rich slurry will be favorable for reducing the regeneration energy consumption. As presented in Figure 7b, the overall energy consumption for 3.0 M ProK/EGME system was found to be about 3300 kJ kg⁻¹ CO₂, with about 7% further reduction by taking advantages of phase separation. About 47% of overall energy consumption was saved in comparison with the baseline case.

To further verify these results, a second way is applied to evaluate the regeneration heat duty excluding the effect of heat dissipation. Some blank systems using the resultant solutions (after desorption) were performed the same desorption

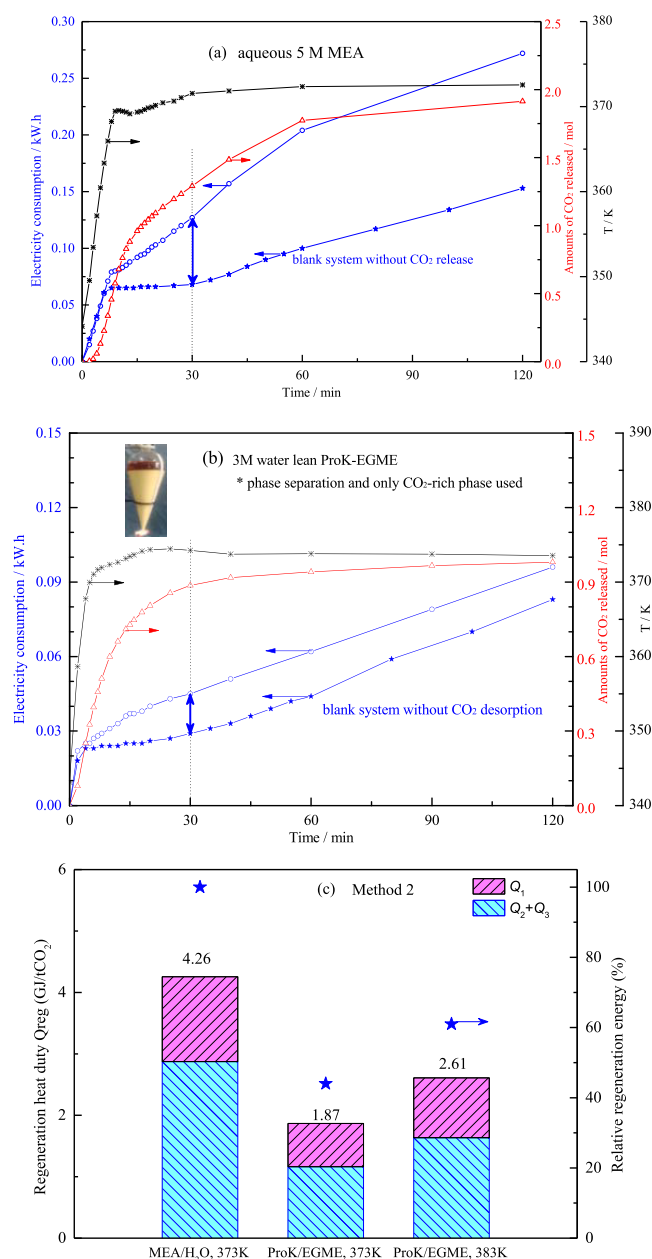


Figure 8. Comparison of energy consumption under thermal desorption conditions at 373 K for CO₂-saturated aqueous and water-lean systems (under 15.0 kPa of CO₂ partial pressure at 313 K). Method 2: Desorption profiles of aqueous 5.0 M MEA (a), 3.0 M ProK/EGME slurry without phase separation and CO₂-rich slurry (b), and comparison of the calculated heat energy requirement Q_{reg} in the first 30 min (c). Note: the blank systems in (a) and (b) are referred to the corresponding desorbed solutions at 373 K for 2 h. Q_1 : estimated sensible heat; $Q_2 + Q_3$: the heat energy required for vaporization of the solvent (Q_2) and CO₂ desorption reaction (Q_3) based on the effective conversion factor 75% for electricity to heat energy.

procedure again and the results are also presented in Figures 8 and S6c,d. The energy required without CO₂ desorption (H_0) for these blank cases, which is associated with sensible heat (Q_1) and heat loss (Q_{loss}). Thus, the sum of heat of vaporization (Q_2) of specific solvent and desorption heat (Q_3) can be obtained from the difference between the overall heat requirement H_T and H_0 . Moreover, the sensible heat (Q_1)

was also estimated by eq 4. ΔT was set to be 10 and 20 K for desorption at 373 and 383 K, respectively, which is an acceptable value of a heat exchanger. The calculated results are summarized in Table S4 and Figure 8c. As can be seen, the heat capacity of the ProK-based phase-change system was much lower than that of aqueous MEA; thus, the sensible heat Q_1 of the 3.0 M ProK/EGME solution was lower than that of aqueous MEA solution. The heat duty of $Q_2 + Q_3$ of aqueous MEA solution was estimated to be 2875 kJ kg⁻¹ CO₂, which is much greater than that (i.e., 1164 kJ kg⁻¹ CO₂) of 3.0 M ProK/EGME solution. The relative Q_{reg} for ProK/EGME solution is found to be only 44% on the basis of the aqueous MEA system (about 4.26 GJ t⁻¹ CO₂). The results can be ascribed to the following three factors. First, removal of CO₂-lean liquid phase can reduce about 30% of the total mass for regeneration and the corresponding sensible heat. Second, EGME has lower specific heat and lower evaporation amount than water at 373 K, which can make a significant contribution to the energy saving. Third, the lower heat of absorption than conventional MEA may result in a further reduction in regeneration energy. Generally, the order of heat of reaction for chemical absorbents is primary amines > secondary amines > carbonates as reported in the literature.^{58–60} Moreover, heat of absorption of CO₂ in the absorbent is similar to the quantity of heat for CO₂ desorption. Both ProK and SarK have one secondary amino group in their molecular structures; thus, the limited solubility of product species in EGME resulted in enrichment of bicarbonate and carbamates in the solid precipitates. Increasing the desorption temperature to 383 K for the slurry ProK/EGME system, the amount of CO₂ released was found to be at the same level with the conventional MEA solution at 373 K. Significant increase in the heat duty of $Q_2 + Q_3$, about 40%, was observed, mainly due to the increasing evaporation amount of EGME and CO₂ desorption efficiency. In this case, there has still about 40% reduction in Q_{reg} compared with the baseline system. Comparison of regeneration energy consumption with other absorbents in literatures was listed in Table S5.

Therefore, these two different methods give consistent results in regeneration energy consumption for water-lean phase change ProK/EGME system. About 40–50% energy reduction indicates that water-lean phase change ProK/EGME system has a great potential as advanced absorbents for energy-efficient CO₂ capture. These water-lean absorbents can be used for CO₂ removal from natural gas processing and biogas upgrading plants considering the issue of water balance. Additionally, using microwaves to regenerate the CO₂-rich solid phase is in progress in our lab for concerning the high efficiency of heat transfer for viscous slurry solutions over the conventional heating. The long-term stability of absorbent at desorption temperature is also worth investigating in future work.

CONCLUSIONS

In summary, we report a novel phase change absorbent containing amino acid salt (ProK or SarK) and 2-alkoxyethanol and investigate its potential in reducing the regeneration energy for CO₂ capture process. Weak polar 2-alkoxyethanols were found to be effective physical antisolvents for liquid-to-solid phase change during CO₂ absorption. For the promising water-lean systems of 3.0 M ProK/EGME and 2.0 M SarK/EGME, about 50–80% of the absorbed CO₂ can be enriched in the solid phase with CO₂ loading in the range of 2.5–3.5

mol kg⁻¹. The 3.0 M ProK/EGME system showed comparable absorption capacity and operating cyclic capacity in comparison with aqueous 5.0 M MEA. Bicarbonate, protonated amino acid and small amount of carbamate salt were proved to be the product species in the solid precipitate by NMR and XRD analysis. The regeneration heat duty for the proposed absorbents was estimated to be 1.87–2.61 GJ/t CO₂, which is about 40–55% lower than aqueous 5.0 M MEA (about 4.26 GJ/t CO₂). Considering enhanced phase separation instead of gravitational settling for 3.0 M ProK/EGME system in practical use, a further reduction of regeneration energy can be expected compared with the baseline case.

■ ASSOCIATED CONTENT

SI Supporting Information

The Supporting Information is available free of charge at <https://pubs.acs.org/doi/10.1021/acssuschemeng.0c03525>.

Schematic diagram of the absorption–desorption and measuring overall energy consumption for solvent regeneration, estimation of the rate of CO₂ absorption and desorption, measurement of CO₂ loading, chemical shift of ¹³C NMR spectra of SarK+EGME and ProK+EGME solution in D₂O, estimation of regeneration energy consumption for various absorbent solutions, DSC-TGA profiles of solid precipitates, desorption profiles for CO₂-saturated aqueous and water-lean systems at 373 K; and Tables S1–S5 and Figures S1–S6 as noted in the text (PDF)

■ AUTHOR INFORMATION

Corresponding Author

Shufeng Shen – School of Chemical and Pharmaceutical Engineering, Hebei University of Science and Technology, Shijiazhuang 050018, P.R. China; orcid.org/0000-0003-0625-133X; Phone: +86 311 88632183; Email: sfshen@hebast.edu.cn, shufengshen@gmail.com; Fax: +86 311 88632183

Authors

Hui Li – School of Chemical and Pharmaceutical Engineering, Hebei University of Science and Technology, Shijiazhuang 050018, P.R. China; orcid.org/0000-0001-9505-4711

Hui Guo – School of Chemical and Pharmaceutical Engineering, Hebei University of Science and Technology, Shijiazhuang 050018, P.R. China

Complete contact information is available at: <https://pubs.acs.org/doi/10.1021/acssuschemeng.0c03525>

Notes

The authors declare no competing financial interest.

■ ACKNOWLEDGMENTS

This work was supported by the Key Program of Hebei Provincial Natural Science Foundation (B2018208154), Hundred Outstanding Innovation Talents in Hebei Universities (SLRC2019051), and Program for Outstanding Talent Engineers of Hebei Province (A2017002022).

■ REFERENCES

- (1) Liu, S.; Ma, R.; Hu, X.; Wang, L.; Wang, X.; Radosz, M.; Fan, M. CO₂ adsorption on hazelnut shell derived nitrogen-doped porous carbons synthesized by single-step sodium amide activation. *Ind. Eng. Chem. Res.* **2020**, *59*, 7046–7053.
- (2) Liu, S.; Rao, L.; Yang, P.; Wang, X.; Wang, L.; Ma, R.; Yue, L.; Hu, X. Superior CO₂ uptake on nitrogen doped carbonaceous adsorbents from commercial phenolic resin. *J. Environ. Sci.* **2020**, *93*, 109–116.
- (3) Chanut, N.; Bourrelly, S.; Kuchta, B.; Serre, C.; Chang, J.-S.; Wright, P. A.; Llewellyn, P. L. Screening the effect of water vapour on gas adsorption performance: Application to CO₂ capture from flue gas in Metal-Organic Frameworks. *ChemSusChem* **2017**, *10*, 1543–1553.
- (4) Mumford, K. A.; Wu, Y.; Smith, K. H.; Stevens, G. W. Review of solvent based carbon-dioxide capture technologies. *Front. Chem. Sci. Eng.* **2015**, *9*, 125–141.
- (5) Vitillo, J. G.; Smit, B.; Gagliardi, L. Introduction: Carbon capture and separation. *Chem. Rev.* **2017**, *117*, 9521–9523.
- (6) Budzianowski, W. M. Explorative analysis of advanced solvent processes for energy efficient carbon dioxide capture by gas-liquid absorption. *Int. J. Greenhouse Gas Control* **2016**, *49*, 108–120.
- (7) Zhang, S.; Lu, Y. Kinetic performance of CO₂ absorption into a potassium carbonate solution promoted with the enzyme carbonic anhydrase: comparison with a monoethanolamine solution. *Chem. Eng. J.* **2015**, *279*, 335–343.
- (8) Lai, Q.; Toan, S.; Assiri, M. A.; Cheng, H.; Russell, A. G.; Adidharma, H.; Radosz, M.; Fan, M. Catalyst-TiO(OH)₂ could drastically reduce the energy consumption of CO₂ capture. *Nat. Commun.* **2018**, *9*, 2672.
- (9) Zhang, X.; Zhang, X.; Liu, H.; Li, W.; Xiao, M.; Gao, H.; Liang, Z. Reduction of energy requirement of CO₂ desorption from a rich CO₂-loaded MEA solution by using solid acid catalysts. *Appl. Energy* **2017**, *202*, 673–684.
- (10) Vericella, J. J.; Baker, S. E.; Stolaroff, J. K.; Duoss, E. B.; Hardin, J. O.; Lewicki, J.; Glogowski, E.; Floyd, W. C.; Valdez, C. A.; Smith, W. L.; Satcher, J. H.; Bourcier, W. L. J.; Spadaccini, C. M.; Lewis, J. A.; Aines, R. D. Encapsulated liquid sorbents for carbon dioxide capture. *Nat. Commun.* **2015**, *6*, 6124.
- (11) Zheng, F.; Heldebrant, D.; Mathias, P.; Koech, P.; Bhakta, M.; Freeman, C.; Bearden, M.; Zwoster, A. Bench-scale testing and process performance projections of CO₂ capture by CO₂-binding organic liquids (CO₂BOLs) with and without polarity-swing-assisted regeneration. *Energy Fuels* **2016**, *30*, 1192–1203.
- (12) Zhang, S.; Shen, Y.; Wang, L.; Chen, J.; Lu, Y. Phase change solvents for post-combustion CO₂ capture: Principle, advances, and challenges. *Appl. Energy* **2019**, *239*, 876–897.
- (13) Ye, J.; Jiang, C.; Chen, H.; Shen, Y.; Zhang, S.; Wang, L.; Chen, J. Novel Biphasic Solvent with Tunable Phase Separation for CO₂ Capture: Role of Water Content in Mechanism, Kinetics, and Energy Penalty. *Environ. Sci. Technol.* **2019**, *53*, 4470–4479.
- (14) Jiang, C.; Chen, H.; Wang, J.; Shen, Y.; Ye, J.; Zhang, S.; Wang, L.; Chen, J. Phase Splitting Agent Regulated Biphasic Solvent for Efficient CO₂ Capture with a Low Heat Duty. *Environ. Sci. Technol.* **2020**, *54*, 7601–7610.
- (15) Shen, Y.; Chen, H.; Wang, J. L.; Zhang, S. H.; Jiang, C. K.; Ye, J. X.; Wang, L. D.; Chen, J. M. Two-stage interaction performance of CO₂ absorption into biphasic solvents: Mechanism analysis, quantum calculation and energy consumption. *Appl. Energy* **2020**, *260*, 114343.
- (16) Zhang, X. P.; Zhang, X. C.; Dong, H. F.; Zhao, Z. J.; Zhang, S. J.; Huang, Y. Carbon capture with ionic liquids: overview and progress. *Energy Environ. Sci.* **2012**, *5*, 6668–6681.
- (17) Liu, F.; Fang, M.; Yi, N.; Wang, T.; Wang, Q. Biphasic behaviors and regeneration energy of a 2-(diethylamino)-ethanol and 2-((2-aminoethyl)amino) ethanol blend for CO₂ capture. *Sustainable Energy Fuels* **2019**, *3*, 3594–3602.
- (18) Xu, Z.; Wang, S.; Chen, C. CO₂ absorption by biphasic solvents: mixtures of 1,4-butanediamine and 2-(diethylamino)-ethanol. *Int. J. Greenhouse Gas Control* **2013**, *16*, 107–115.
- (19) Ye, Q.; Wang, X.; Lu, Y. Screening and evaluation of novel biphasic solvents for energy-efficient post-combustion CO₂ capture. *Int. J. Greenhouse Gas Control* **2015**, *39*, 205–214.

- (20) Wang, L.; Zhang, Y.; Wang, R.; Li, Q.; Zhang, S.; Li, M.; Liu, J.; Chen, B. Advanced Monoethanolamine Absorption Using Sulfolane as a Phase Splitter for CO₂ Capture. *Environ. Sci. Technol.* **2018**, *52*, 14556–14563.
- (21) Luo, W.; Guo, D.; Zheng, J.; Gao, S.; Chen, J. CO₂ absorption using biphasic solvent: Blends of diethylenetriamine, sulfolane and water. *Int. J. Greenhouse Gas Control* **2016**, *53*, 141–148.
- (22) Wang, R.; Liu, S.; Wang, L.; Li, Q.; Zhang, S.; Chen, B.; Jiang, L.; Zhang, Y. Superior energy-saving splitter in monoethanolamine-based biphasic solvents for CO₂ capture from coal-fired flue gas. *Appl. Energy* **2019**, *242*, 302–310.
- (23) Yang, F.; Jin, X.; Fang, J.; Tu, W.; Yang, Y.; Cui, C.; Zhang, W. Development of CO₂ phase change absorbents by means of cosolvent effect. *Green Chem.* **2018**, *20*, 2328–2336.
- (24) Barzagli, F.; Mani, F.; Peruzzini, M. Novel water-free biphasic absorbents for efficient CO₂ capture. *Int. J. Greenhouse Gas Control* **2017**, *60*, 100–109.
- (25) Machida, H.; Ando, R.; Esaki, T.; Yamaguchi, T.; Horizoe, H.; Kishimoto, A.; Akiyama, K.; Nishimura, M. Low temperature swing process for CO₂ absorption-desorption using phase separation CO₂ capture solvent. *Int. J. Greenhouse Gas Control* **2018**, *75*, 1–7.
- (26) Barzagli, F.; Mani, F.; Peruzzini, M. Efficient CO₂ absorption and low temperature desorption with non-aqueous solvents based on 2-amino-2-methyl-1-propanol (AMP). *Int. J. Greenhouse Gas Control* **2013**, *16*, 217–223.
- (27) Zheng, S.; Tao, M.; Liu, Q.; Ning, L.; He, Y.; Shi, Y. Capturing CO₂ into the precipitate of a phase-changing solvent after absorption. *Environ. Sci. Technol.* **2014**, *48*, 8905–8910.
- (28) Tao, M.; Gao, J.; Zhang, W.; Li, Y.; He, Y.; Shi, Y. A novel phase-changing nonaqueous solution for CO₂ capture with high capacity, thermostability, and regeneration efficiency. *Ind. Eng. Chem. Res.* **2018**, *57*, 9305–9312.
- (29) Zhang, Z.; Zhao, W.; Nong, J.; Feng, D.; Li, Y.; Chen, Y.; Chen, J. Liquid-solid phase-change behavior of diethylenetriamine in nonaqueous systems for carbon dioxide absorption. *Energy Technol.* **2017**, *5*, 461–468.
- (30) Zhao, W. B.; Zhao, Q.; Zhang, Z.; Liu, J. J.; Chen, R.; Chen, Y.; Chen, J. Liquid-solid phase-change absorption of acidic gas by polyamine in nonaqueous organic solvent. *Fuel* **2017**, *209*, 69–75.
- (31) Li, Y.; Cheng, J.; Hu, L.; Liu, J.; Zhou, J.; Cen, K. Phase-changing solution PZ/DMF for efficient CO₂ capture and low corrosiveness to carbon steel. *Fuel* **2018**, *216*, 418–426.
- (32) Shen, S.; Bian, Y.; Zhao, Y. Energy-efficient CO₂ capture using potassium proline/ethanol solution as a phase-changing absorbent. *Int. J. Greenhouse Gas Control* **2017**, *56*, 1–11.
- (33) Majchrowicz, M. E.; Kersten, S.; Brilman, W. Reactive absorption of carbon dioxide in L-proline salt solutions. *Ind. Eng. Chem. Res.* **2014**, *53*, 11460–11467.
- (34) Shen, S.; Yang, Y.; Wang, Y.; Ren, S.; Han, J.; Chen, A. CO₂ absorption into aqueous potassium salts of lysine and proline: density, viscosity and solubility of CO₂. *Fluid Phase Equilib.* **2015**, *399*, 40–49.
- (35) Aronu, U. E.; Hartono, A.; Hoff, K. A.; Svendsen, H. F. Kinetics of carbon dioxide absorption into aqueous amino acid salt: potassium salt of sarcosine solution. *Ind. Eng. Chem. Res.* **2011**, *50*, 10465–10475.
- (36) Zhao, Y.; Bian, Y.; Li, H.; Guo, H.; Shen, S.; Han, J.; Guo, D. A comparative study of aqueous potassium lysinate and aqueous monoethanolamine for postcombustion CO₂ capture. *Energy Fuels* **2017**, *31*, 14033–14044.
- (37) Holst, J. v.; Versteeg, G. F.; Brilman, D. W. F.; Hogendoorn, J. A. Kinetic study of CO₂ with various amino acid salts in aqueous solution. *Chem. Eng. Sci.* **2009**, *64*, 59–68.
- (38) Li, C.; Zhao, Y.; Shen, S. Aqueous potassium lysinate for CO₂ capture: Evaluating at desorber conditions. *Energy Fuels* **2019**, *33*, 10090–10098.
- (39) Shen, S.; Yang, Y.; Bian, Y.; Zhao, Y. Kinetics of CO₂ absorption into aqueous basic amino acid salt: potassium salt of lysine solution. *Environ. Sci. Technol.* **2016**, *50*, 2054–2063.
- (40) Sanchez Fernandez, E.; Heffernan, K.; Van Der Ham, L. V.; Linders, M. J. G.; Eggink, E.; Schrama, F. N. H.; Brilman, D. W. F.; Goetheer, E. L. V.; Vlucht, T. J. H. Conceptual Design of a Novel CO₂ Capture Process Based on Precipitating Amino Acid Solvents. *Ind. Eng. Chem. Res.* **2013**, *52*, 12223–12235.
- (41) Raksajati, A.; Ho, M. T.; Wiley, D. E. Understanding the impact of process design on the cost of CO₂ capture for precipitating solvent absorption. *Ind. Eng. Chem. Res.* **2016**, *55* (7), 1980–1994.
- (42) Aronu, U. E.; Ciftja, A. F.; Kim, I.; Hartono, A. Understanding Precipitation in Amino Acid Salt Systems at Process Conditions. *Energy Procedia* **2013**, *37*, 233–240.
- (43) Bian, Y.; Shen, S. CO₂ absorption into a phase change absorbent: water-lean potassium proline/ethanol solution. *Chin. J. Chem. Eng.* **2018**, *26*, 2318–2326.
- (44) Guo, H.; Li, H.; Shen, S. CO₂ capture by water-lean amino acid salts: absorption performance and mechanism. *Energy Fuels* **2018**, *32*, 6943–6954.
- (45) Alivand, M. S.; Mazaheri, O.; Wu, Y.; Stevens, G. W.; Scholes, C. A.; Mumford, K. A. Development of aqueous-based phase change amino acid solvents for energy-efficient CO₂ capture: The role of antisolvent. *Appl. Energy* **2019**, *256*, 113911.
- (46) Lide, D. R., Ed.; *CRC Handbook of chemistry and physics*, 90th ed.; CRC Press: Boca Raton, FL, 2010.
- (47) Lechner, M. D., Ed.; *Static Dielectric Constants of Pure Liquids and Binary Liquid Mixtures (Supplement to Vol. IV/17)*; Springer-Verlag: Berlin, 2008.
- (48) Guo, H.; Shi, X.; Shen, S. Solubility of N₂O and CO₂ in nonaqueous systems of monoethanolamine and glycol ethers: Measurements and model representation. *J. Chem. Thermodyn.* **2019**, *137*, 76–85.
- (49) Guo, H.; Li, C. X.; Shi, X. Q.; Li, H.; Shen, S. F. Nonaqueous amine-based absorbents for energy efficient CO₂ capture. *Appl. Energy* **2019**, *239*, 725–734.
- (50) Guo, H.; Hui, L.; Shen, S. Monoethanolamine+2-methoxyethanol mixtures for CO₂ capture: Density, viscosity and CO₂ solubility. *J. Chem. Thermodyn.* **2019**, *132*, 155–163.
- (51) Luo, X.; Liu, S.; Gao, H.; Liao, H.; Tontiwachwuthikul, P.; Liang, Z. An improved fast screening method for single and blended amine-based solvents for post-combustion CO₂ capture. *Sep. Purif. Technol.* **2016**, *169*, 279–288.
- (52) Hartono, A.; Vevelstad, S. J.; Ciftja, A.; Knuutila, H. K. Screening of strong bicarbonate forming solvents for CO₂ capture. *Int. J. Greenhouse Gas Control* **2017**, *58*, 201–211.
- (53) Li, C.; Shi, X.; Shen, S. Performance evaluation of newly developed absorbents for solvent-based carbon dioxide capture. *Energy Fuels* **2019**, *33*, 9032–9039.
- (54) Oh, S. Y.; Binns, M.; Cho, H.; Kim, J. K. Energy minimization of MEA-based CO₂ capture process. *Appl. Energy* **2016**, *169*, 353–362.
- (55) Perinu, C.; Arstad, B.; Jens, K. J. NMR spectroscopy applied to amine-CO₂-H₂O systems relevant for post-combustion CO₂ capture: A review. *Int. J. Greenhouse Gas Control* **2014**, *20*, 230–243.
- (56) Hartono, A.; Aronu, U. E.; Svendsen, H. F. Liquid speciation study in amine amino acid salts for CO₂ absorbent with ¹³C-NMR. *Energy Procedia* **2011**, *4*, 209–215.
- (57) Ciftja, A. F.; Hartono, A.; Svendsen, H. F. ¹³C NMR as a method species determination in CO₂ absorbent systems. *Int. J. Greenhouse Gas Control* **2013**, *16*, 224–232.
- (58) Chowdhury, F. A.; Okabe, H.; Yamada, H.; Onoda, M.; Fujioka, Y. Synthesis and selection of hindered new amine absorbents for CO₂ capture. *Energy Procedia* **2011**, *4*, 201–208.
- (59) Machida, H.; Oba, K.; Tomikawa, T.; Esaki, T.; Yamaguchi, T.; Horizoe, H. Development of phase separation solvent for CO₂ capture by aqueous (amine + ether) solution. *J. Chem. Thermodyn.* **2017**, *113*, 64–70.
- (60) Kim, I.; Svendsen, H. F. Heat of absorption of carbon dioxide (CO₂) in monoethanolamine (MEA) and 2-(aminoethyl)-ethanolamine (AEEA) solutions. *Ind. Eng. Chem. Res.* **2007**, *46*, 5803–5809.